Catalytic influence of underpotentially deposited submonolayers of different metals in ethylene glycol oxidation on various noble metal electrodes in alkaline medium

A.A. El-Shafei, H.M. Shabanah and M.N.H. Moussa
Chemistry Department, Faculty of Science, El-Mansoura University, El-Mansoura (Egypt)

(Received November 23, 1992; in revised form April 7, 1993; accepted April 30, 1993)

Abstract

The electrochemical oxidation of ethylene glycol has been studied on Pt, Pd and Au electrodes in alkaline medium in the absence and in the presence of metal ad-atoms. For pure-metal electrodes, the maximum current density was obtained at an Au electrode. However, in the presence of metal ad-atoms, enhancement of catalytic activity changes its order to: Pt > Au > Pd. The three different electrodes exhibit maximum catalytic activity when modified with Pb ad-atoms. The decreasing order of enhancement by ad-atoms under investigation is: Pb > Bi > Tl > Sn > Cd.

Introduction

The original interest in the anodic oxidation of aliphatic alcohols was in their possible application in fuel cells [1]. One of them, ethylene glycol (EG), seems to be a very attractive fuel for alkaline fuel cells. This is due to its high reactivity, particularly on gold electrodes [2, 3]. However, oxalate – produced as a result of the complete oxidation of ethylene glycol – needs to be removed from the alkaline electrolyte [4, 5]. In addition, ethylene glycol was considered as a suitable fuel for use at higher temperatures [6, 7].

Several reaction mechanisms for EG electrooxidation on Pt substrates in acidic [8–12] as well as in alkaline media [13, 14] have been proposed but the nature of adsorbed residues, which poison the electrode surface, is still under discussion. The electrocatalytic oxidation of EG on modified Pt substrates has been studied both in acidic [15–17] and in alkaline [18] solutions. Recently, the electrooxidation of EG on an Au electrode in acidic and in alkaline media has been studied [2, 3]. In acidic medium Au behaves as a poor electrocatalyst whereas it is an excellent electrocatalyst, even much better than Pt, in alkaline medium. This difference was explained by the different modes of adsorption of polyols on Pt and Au surfaces.

In the present work, the effect of underpotentially deposited (UPD) ad-atoms (Pb, Bi, Tl, Sn, Cd) on the catalytic activity of some noble metal electrodes (Pt, Pd, Au) towards the electrooxidation of EG in alkaline media is studied by cyclic voltammetry and potential step techniques.

0378-7753/93/$6.00

Experimental

The electrooxidation of EG was examined by cyclic voltammetry and potential step techniques as previously described [19]. Pt and Au sheets served as counter electrodes. Potentials were measured versus an Ag/AgCl/saturated KNO_3 electrode. The working electrodes were Pt, Pd and Au sheets modified by UPD of foreign metal ad-atoms. The UPD of the different metal ad-atoms was obtained by adding the corresponding salts – $Pb(ClO_4)_2 \cdot 3H_2O$ (Aldrich), $Bi(NO_3)_3 \cdot 5H_2O$ (BDH), $TlNO_3$ (Prolabo), $SnSO_4$ (BDH), $CdSO_4 \cdot 8/3H_2O$ (Ridel–de Haen) – at low concentrations (10^{-7}–5×10^{-5} M) to the electrolytic solution. The electrolytic solution (0.1 M CH_2OH–CH_2OH (BDH) in 0.1 M NaOH (BDH) was prepared with megapure water. All solutions were purged with purified nitrogen (99.996%).

The real surface area was determined from the hydrogen region for Pt electrodes [20] and from the oxygen reduction peak for Au and Pd electrodes [21, 22] in the voltammograms recorded in a sulfuric acid (BDH) electrolyte.

Results and discussion

Oxidation of EG on modified Pt electrode

The UPD of Pb, Bi, Tl, Sn and Cd on the Pt electrode in alkaline media has been previously described [18, 23]. The voltammograms of a Pt electrode recorded in the absence and in the presence of metal salts are given in Fig. 1. UPD ad-layers of Pb are formed on the electrode surface according to the reaction:

$$HPbO_2^- + H_2O + 2e^- \longrightarrow Pb_{ads.} + 3OH^- \tag{1}$$

The UPD of Pb begins in the negative potential sweep at -0.2 V, while its redissolution starts at ~ -0.3 V, with a main desorption peak at -0.22 V. Tl^+ ions are underpotentially deposited on Pt in the negative potential scan between ~ -0.1 V and -0.8 V, giving various reduction peaks depending on the Tl^+ ion concentrations. Its redissolution during the positive sweep also gives several oxidation peaks at potentials more positive than -0.5 V. The main UPD peak of Bi appears at -0.37 V and the main redissolution peak at -0.18 V. The UPD of Cd occurs during the negative sweep in a single peak at -0.39 V; the redissolution reaction takes place in a broad peak at ~ -0.1 V. Sn is underpotentially deposited in strong alkaline medium according to the reaction:

$$SnO_2^{2-} + 2H_2O + 2e^- \longrightarrow Sn_{ads.} + 4OH^- \tag{2}$$

The UPD of Sn occurs in the negative sweep in a single peak at -0.35 V. The main redissolution peak occurs at -0.15 V.

The effect of submonolayers of different ad-atoms on EG oxidation on a Pt electrode has been studied previously [18]. However, the effect of some metal ad-atoms was examined under the present experimental conditions in order to compare their influence on the three noble metal electrodes towards EG oxidation. Figures 2 and 3 show the cyclic voltammograms and steady-state polarization curves of EG oxidation on bare Pt and on Pt surfaces modified by UPD submonolayers of Pb, Bi, Tl, Sn and Cd in 0.1 M NaOH.

The oxidation of EG on a Pt electrode is strongly enhanced by the presence of Pb, Bi and Tl ad-atoms. The general shape of the oxidation curves is unchanged, but the current densities are greatly magnified, reaching about 14 mA/cm^2 in the positive scan for 1×10^{-4} M Pb^{2+} in solution. The presence of Sn ad-atoms at the optimum

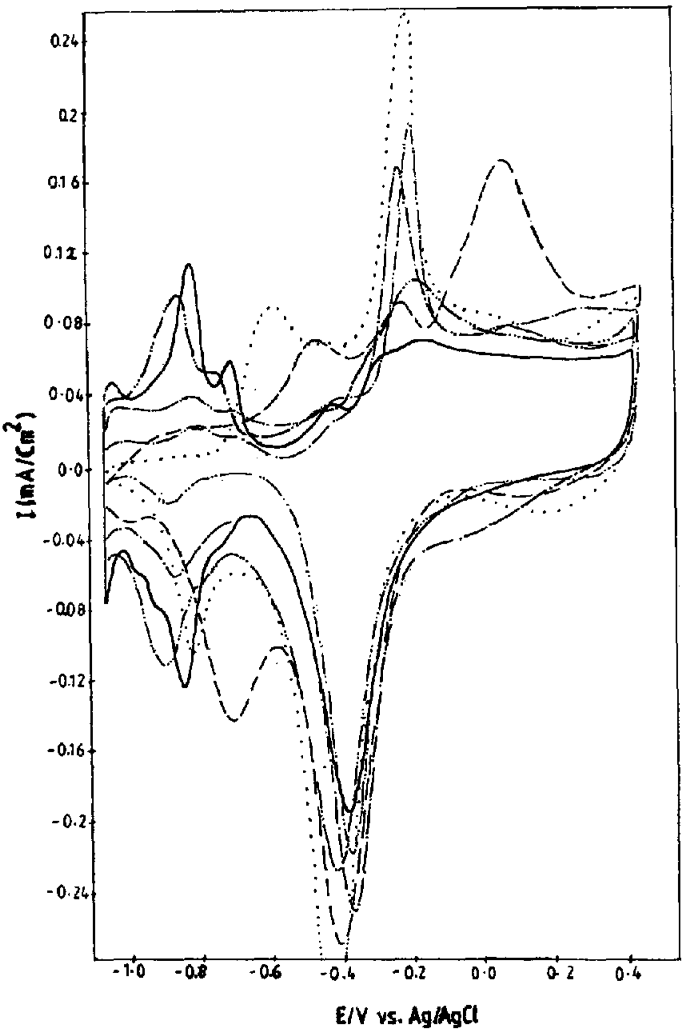

Fig. 1. Cyclic voltammograms of Pt electrodes in 0.1 M NaOH (——) in the absence and in the presence of (–·–) 1×10^{-5} M Pb^{2+}, (·····) 10^{-5} M Bi^{3+}, (– – –) 5×10^{-5} M Tl^{+}, (–··–) 1×10^{-6} M Sn^{2+} and (–···–) 5×10^{-5} M Cd^{2+}; sweep rate 100 mV/s at 25 °C.

concentration (5×10^{-6} M Sn^{2+} in solution) only slightly increases the current density without changing the shape of the voltammogram. The oxidation rate of EG in the presence of Cd ad-atoms slightly increases during the positive sweep at the optimum concentration (5×10^{-7} M Cd^{2+} in solution). For concentrations $>1\times10^{-6}$ M Cd^{2+}, the current density is slightly smaller than on a pure Pt electrode. However, Cd ad-atoms shift the current–potential curves towards a more negative potential. The catalytic activity decreases in the following order: Pb > Bi > Tl > Sn > Cd (Fig. 3).

Oxidation of EG on modified Pd electrode

The voltammograms of Pb, Bi, Tl, Sn and Cd on Pd electrodes in alkaline medium, together with that of pure Pd surfaces are shown in Fig. 4. The UPD of Pb begins

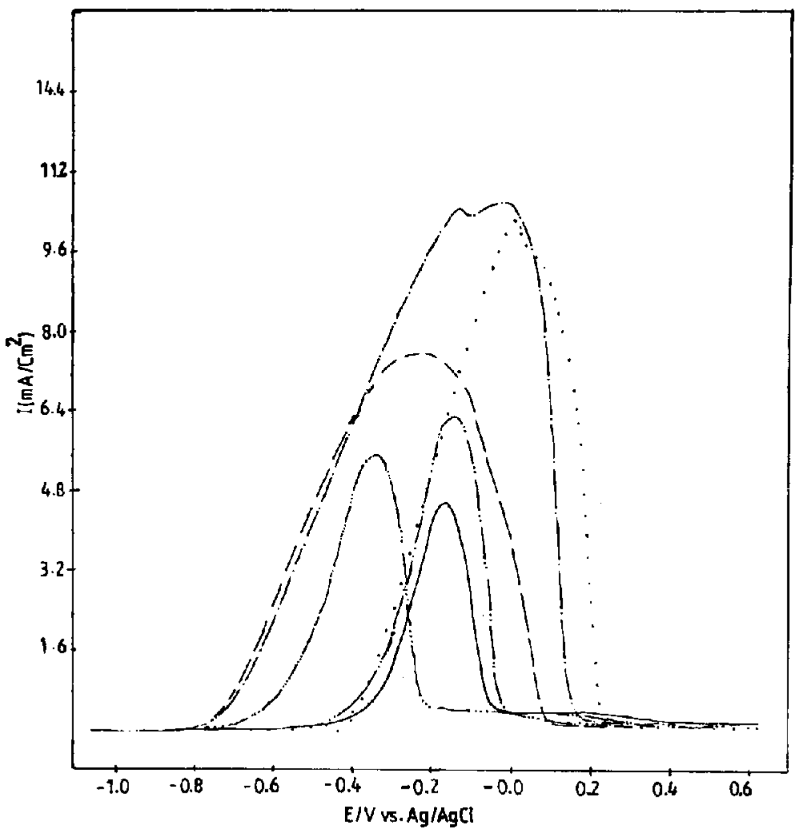

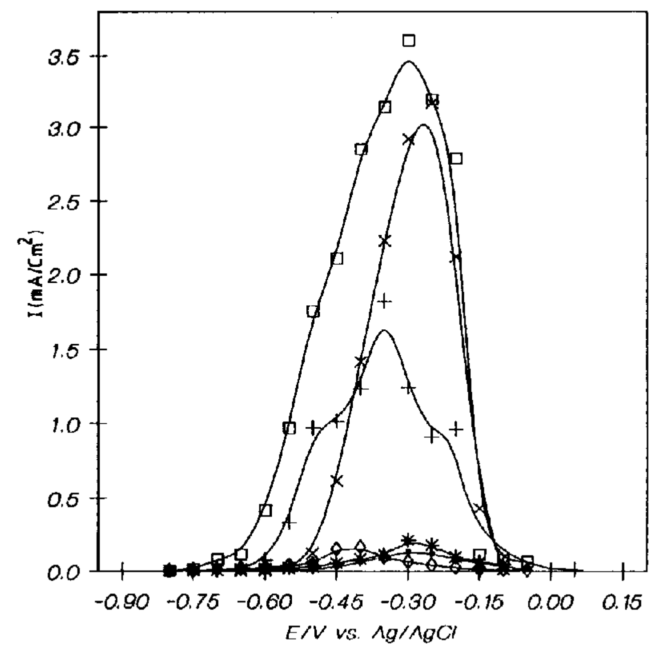

Fig. 2. Anodic cyclic voltammograms of Pt electrodes in 0.1 M NaOH containing 0.1 M EG (——) in the absence and in the presence of (–·–) 5×10^{-5} M Pb^{2+}, (·····) 5×10^{-6} M Bi^{3+}, (– – –) 5×10^{-6} M Tl^{+}, (–···–) 5×10^{-6} M Sn^{2+}, and (–····–) 5×10^{-7} M Cd^{2+}; sweep rate 100 mV/s at 25 °C.

Fig. 3. Steady-state polarization curves of 0.1 M EG in 0.1 M NaOH at Pt electrodes at 25 °C: (–■–) free Pt; (–+–) 1×10^{-6} M Tl^{+}; (–∗–) 1×10^{-6} M Sn^{2+}; (–□–) 5×10^{-6} M Pb^{2+}; (–×–) 5×10^{-6} M Bi^{3+}, and (–◇–) 1×10^{-7} M Cd^{2+}.

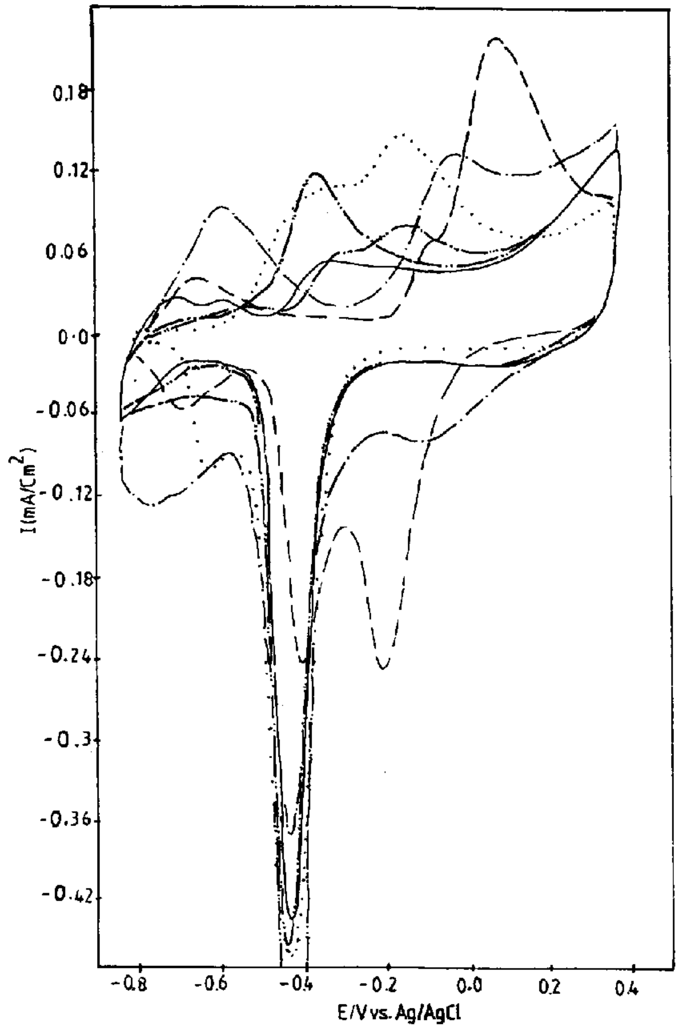

Fig. 4. Cyclic voltammograms of Pd electrodes in 0.1 M NaOH (——) in the absence and in the presence of (-··-) 2.5×10^{-4} M Pb^{2+}, (·····) 1×10^{-5} M Bi^{3+}, (– – –) 5×10^{-5} M Tl^{+}, (– · · · –) 5×10^{-5} M Sn^{2+}, and (– · · · –) 1×10^{-5} M Cd^{2+}; sweep rate 100 mV/s at 25 °C.

in the negative potential sweep at +0.2 V, while the redissolution of the UPD layer starts at ~ −0.7 V, with a main desorption peak at −0.03 V. Tl^+ ions are underpotentially deposited on Pd in the negative scan between 0.0 and −0.75 V, giving various reduction peaks, that depend on the Tl^+ ion concentrations in the solution. The UPD layer redissolution in the positive sweep starts at 0.15 V, with several oxidation peaks at −0.7 and +0.1 V. The UPD of Bi ad-atoms takes place according to the reaction:

$$BiO_2^- + 2H_2O + 3e^- \longrightarrow Bi_{ads.} + 4OH^- \qquad (3)$$

or,

$$BiO^+ + H_2O + 3e^- \longrightarrow Bi_{ads.} + 2OH^- \qquad (4)$$

which occurs together with palladium oxide reduction. Its redissolution begins at −0.55 V, giving two desorption peaks at −0.35 and −0.15 V, respectively. The UPD of Sn ad-atoms is realized from the soluble species SnO_2^{2-} dissolved in the electrolyte solution. During the negative sweep the UPD begins at −0.45 and extends as far as −0.8 V. The redissolution of Sn during the positive sweep gives a main peak at −0.36 V. The UPD of Cd occurs during the negative sweep between −0.45 and −0.8 V, while its redissolution begins at −0.4 V giving two oxidation peaks at −0.32 and −0.17 V.

The electrooxidation of EG on a Pd electrode is markedly improved by the formation of Pb, Bi and Tl submonolayers on the electrocatalytic surface (Fig. 5). For the optimum concentrations, the current densities at the peak potential during the positive sweep reach values close to 6, 5 and 4 mA/cm² for 1×10^{-5} M Pb^{2+}, 1×10^{-6} M Bi^{3+} and 1×10^{-6} M Tl^{+}, respectively. As in the case of Pt electrodes, Sn and Cd submonolayers lead only to a small increase of the current densities. This increase of current is accompanied by a shift of the polarization curve to a more negative potential for Pd electrode modified by Cd ad-atoms. The catalytic activity

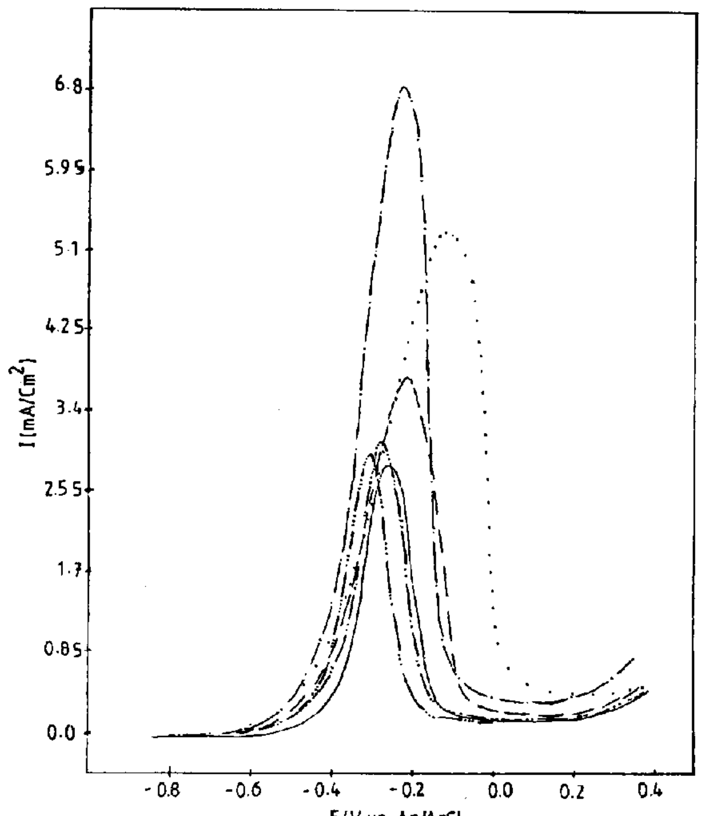

Fig. 5. Anodic cyclic voltammograms of Pd electrodes in 0.1 M NaOH containing 0.1 M EG (——) in the absence and in the presence of (–·–) 1×10^{-6} M Pb^{2+}, (·····) 1×10^{-6} M Bi^{3+}, (– – –) 1×10^{-7} M Tl^{+}, (–···–) 1×10^{-5} M Sn^{2+}, and (–···–) 1×10^{-7} M Cd^{2+}; sweep rate 100 mV/s at 25 °C.

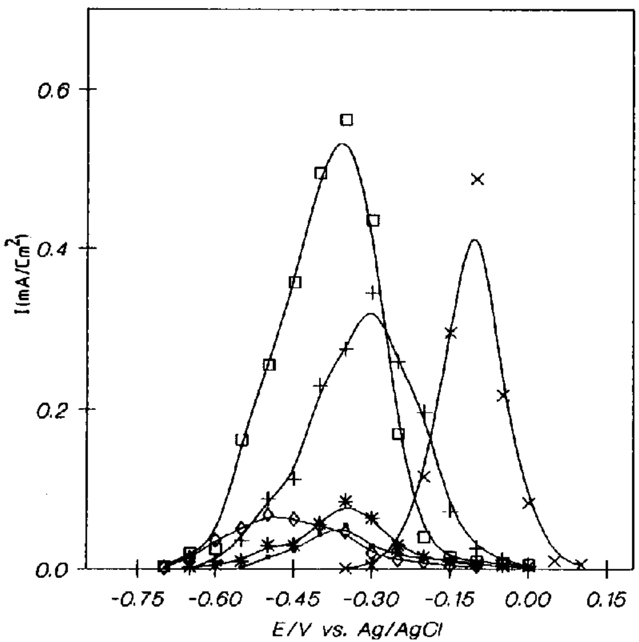

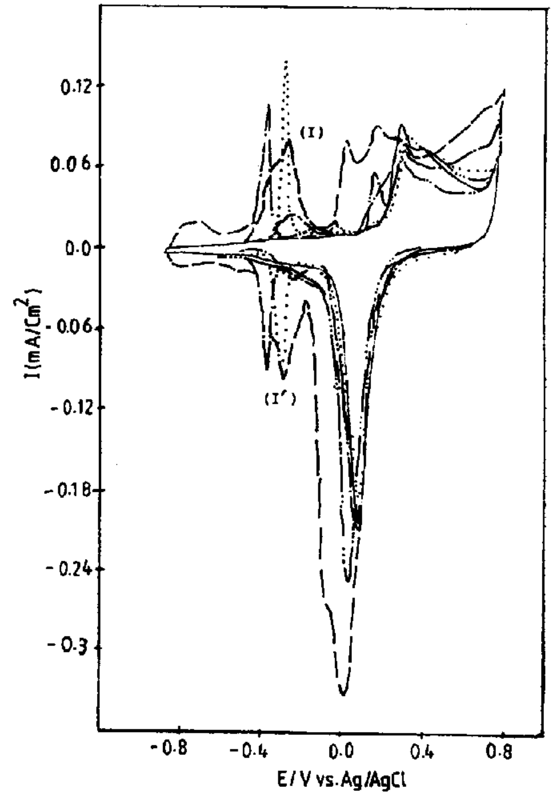

Fig. 6. Steady-state polarization curves of 0.1 M EG in 0.1 M NaOH at Pd electrodes at 25 °C: (-■-) free Pd; (-+-) 5×10^{-6} M Tl^+; (-*-) 5×10^{-6} M Sn^{2+}; (-□-) 1×10^{-6} M Pb^{2+}; (-×-) 5×10^{-6} M Bi^{3+}, and (-◇-) 1×10^{-7} M Cd^{2+}.

Fig. 7. Cyclic voltammograms of Au electrodes in 0.1 M NaOH (——) in the absence and in the presence of (-·-) 1×10^{-5} M Pb^{2+}, (·····) 1×10^{-6} M Bi^{3+}, (---) 5×10^{-5} M Tl^+, (-···-) 1×10^{-6} M Sn^{2+}, and (-····-) 1×10^{-6} M Cd^{2+}; sweep rate 100 mV/s at 25 °C.

decreases following the same order as in the case of Pt electrode. These results are consistent with those obtained under steady-state conditions (Fig. 6).

Oxidation of EG on modified Au electrode

Figure 7 shows the voltammograms recorded for Au electrodes in the absence and the presence of Pb, Bi, Tl, Sn and Cd ions in solution. The UPD of Pb^{2+} occurs in the negative sweep direction from -0.15 to -0.8 V giving different peaks depending on the Pb^{2+} ion concentrations. The main deposition peak is observed at -0.48 V whereas that of redissolution occurs at -0.5 V. Only one reduction peak at -0.36 V and one oxidation peak at -0.34 V are observed for Bi at low concentration (1×10^{-6} M Bi^{3+}). For concentrations $>1\times10^{-5}$ M more complicated voltammograms are obtained. In the presence of $TlNO_3$, the voltammograms of the Au electrode display a rather complicated pattern with several UPD and redissolution peaks. The peaks I and I′ appear to be the principal UPD peaks corresponding to the conversion

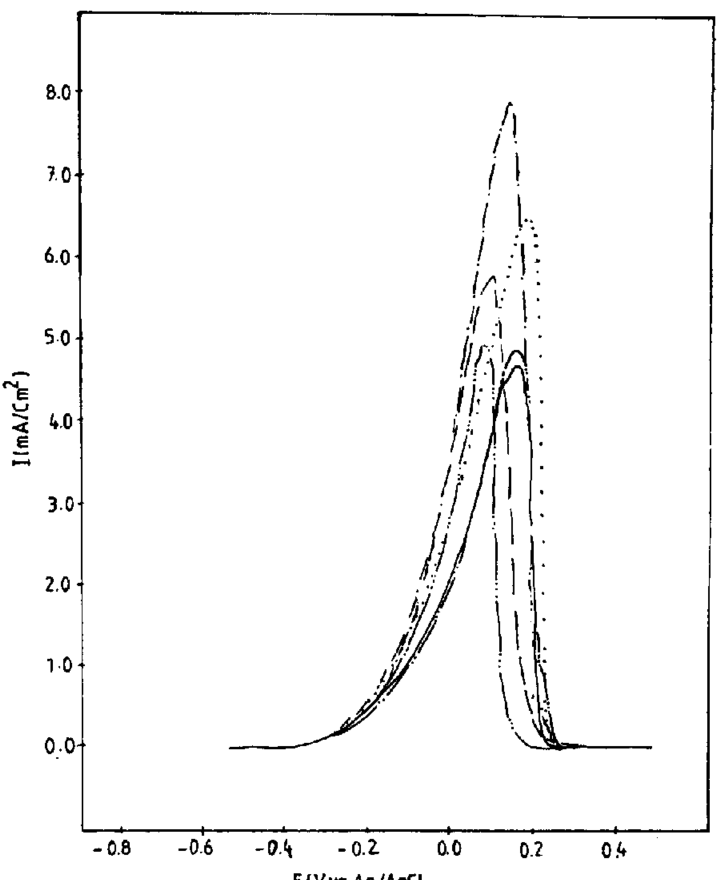

Fig. 8. Anodic cyclic voltammograms of Au electrodes in 0.1 M NaOH containing 0.1 M EG (——) in the absence and in the presence of (–·–) 1×10^{-6} M Pb^{2+}, (·····) 5×10^{-7} M Bi^{3+}, (– – –) 1×10^{-7} M Tl^{+}, (–···–) 1×10^{-6} M Sn^{2+}, and (–····–) 5×10^{-7} M Cd^{2+}; sweep rate 100 mV/s at 25 °C.

of an adsorbed form of Tl(I) to Tl(UPD) and vice versa [24]. The UPD of Sn^{2+} and of Cd^{2+} ions occurs in the negative direction after the oxygen reduction peak, giving a small deposition peak at −0.34 V.

Figures 8 and 9 show the voltammograms and the polarization curves obtained for EG oxidation on an Au electrode modified by UPD of Pb, Bi, Tl, Sn and Cd. The voltammogram obtained at pure Au electrode is given in the same Fig. for comparison. The presence of $HPbO_2^-$, Tl^+ and BiO_2^- (or BiO^+) ions in solution, and their reduction to form UPD ad-layers, result in a significant enhancement of the catalytic activity of the Au electrode for EG oxidation. As in case of Pt and Pd electrodes, catalytic activity decreases in the order: Pb > Bi > Tl. A small increase in current around the peak potential is observed in the presence of Sn ad-atoms. Cd ad-atoms shift the polarization curves to more negative potentials. This can be attributed to their ionic character [25].

For pure-metal electrodes, Au exhibits the highest current density as shown in Fig. 10. This result is consistent with that reported in the literature [2, 3]. However, in the presence of metal ad-atoms the maximum current was obtained at the Pt electrode. In a comparative study between nobel metal electrodes towards the oxidation of HCOOH [26] in acidic medium and D-glucose in alkaline medium [27], a so-called Volcano curve was obtained when the latent heat of sublimation was plotted against log $2(i_p)$. At the apex of the curve lies Pt, which is therefore the best electrocatalyst in this case. The current of the anodic peak is multiplied by two just because the maximum catalytic action appears at coverages $\Theta_M = 0.5$, where half of the active sites on the electrode surface are available for the oxidation of HCOOH and D-glucose. This assumption is in contrast with the following: (i) the optimum coverage by UPD

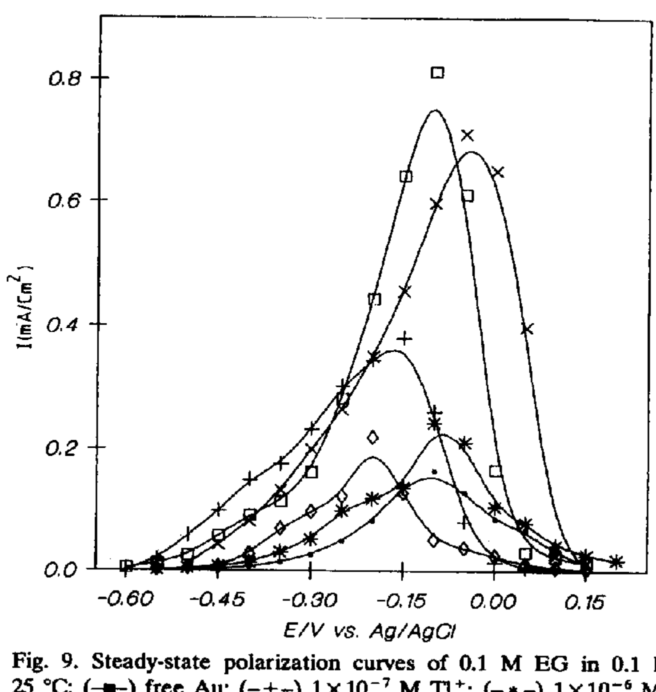

Fig. 9. Steady-state polarization curves of 0.1 M EG in 0.1 M NaOH at Au electrodes at 25 °C: (-■-) free Au; (-+-) 1×10^{-7} M Tl^+; (-*-) 1×10^{-6} M Sn^{2+}; (-□-) 1×10^{-6} M Pb^{2+}; (-×-) 1×10^{-6} M Bi^{3+}, and (-◇-) 1×10^{-7} M Cd^{2+}.

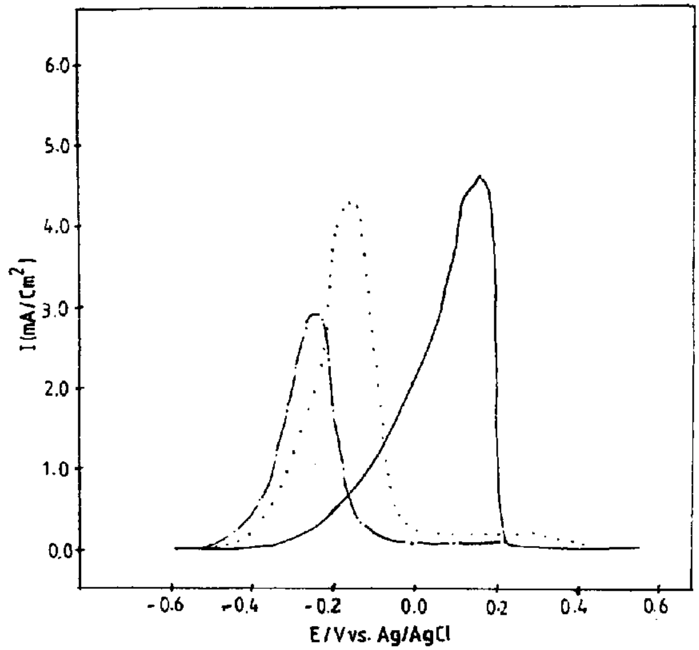

Fig. 10. Voltammetry curves of 0.1 M EG in 0.1 M NaOH at 25 °C; dE/dt = 100 mV/s; (·····) Pt; (——) Au, and (–·–) Pd.

submonolayers is not exactly 0.5 for all the ad-atoms and (ii) the authors assumed that the reaction takes place only on Pt sites free from metal$_{ads.}$. However, Vielstich and collaborators [28], concluded that the oxidation of HCOOH takes place on the Pt surface covered by a monolayer of Pb. The current obtained at an Au electrode was not subjected to multiplication by a factor of two [26], because the UPD of Pb on Au electrode is cathodic to the region where the oxidation of HCOOH on Au takes place. If we apply the rules proposed by Adzic *et al.* [26], a similar order of catalytic activity is obtained (Pt > Pd > Au). Another order is obtained (Pt > Au > Pd) when the actual experimental current values were taken without the above modification and taking into account Vielstich's conclusion. However, in both cases, maximum catalytic activity is found for the Pt electrode modified with UPD submonolayers, especially that modified with Pb ad-atoms.

The effect of the different metal ad-atoms studied here on the electrooxidation rate of EG can be explained by means of the modification of $\Theta_{org.}$ and/or Θ_{OH}, the coverages of organic adsorption residue and adsorbed hydroxyl, respectively, by the foreign metal atoms. The catalytic influence of Pb, Bi and Tl can be attributed to the liberation of free Pt, Pd or Au sites before the EG oxidation, due to the redissolution of the bulk metals (around −0.5 V versus Ag/AgCl/KNO_3) which are able to adsorb EG molecules. At more positive potentials, hydroxyl radicals can be adsorbed on the few metal ad-atoms remaining at the electrode surface. Cd ad-atoms shift the polarization curves to more negative potentials than on pure-metal electrodes [15, 18, 23, 29]. Cd ad-atoms display some ionic character [25]. Sn ad-atoms do not change the polarization curves because this metal does not greatly change the coverage of the adsorbed species; redissolution for Sn ad-atoms occurs in the potential range for EG oxidation.

Acknowledgement

The author thanks Prof Dr W. Vielstich for his donation of the flow cell.

List of symbols

UPD	underpotential deposition
ad-atoms	adsorbed atoms
Θ_M	surface coverage with metal ad-atoms
Θ_{OH}	surface coverage with OH
$\Theta_{org.}$	surface coverage with organic residue
i_p	peak current

References

1 J.O.M. Bockris and S. Srinivasan (eds.), *Fuel Cells*, McGraw-Hill, New York, 1969.
2 B. Beden, I. Cetin, A. Kahyaoglu, D. Takky and C. Lamy, *J. Catalys., 104* (1987) 37–46.
3 O. Enea and J.P. Ango, *Electrochim. Acta, 34* (1989) 391–397.
4 H. Ewe, E. Justi and M. Pesditschek, *Energy Convers., 15* (1975) 9.
5 H. Cnobloch, D. Groppel, H. Kohlmuller, D. Kuhl and G. Siemsen, in J. Thomson (ed.), *Power Sources 7, Proc. 11th Symp., Brighton, UK, 1978*, p. 389.
6 H. Spengler and G. Gruneberg, *DECHEMA-Monogr., 38* (1961) 579–599.
7 G. Gruneberg, J. Kubisch and H. Spengler, *Ger. Pat. Appl. No. 1 163 412* (1958).
8 J. Weber, Yu.B. Vasil'ev and V.S. Bagotskii, *Elektrokhimiya, 2* (1966) 515–521.
9 V.S. Bagotskii and Yu.B. Vasil'ev, *Electrochim. Acta, 11* (1966) 1439–1461.
10 B.I. Podlovchenko and V.F. Stenin, *Elektrokhimiya, 3* (1967) 649–653.
11 A.K. Vijh, *Can. J. Chem., 49* (1971) 78–88.
12 G. Horanyi, V.E. Kazarinov, Yu.B. Vasil'ev and V.N. Andreev, *J. Electroanal. Chem., 147* (1983) 263–278.
13 W. Hauffe and J. Heitbaum, *Electrochim. Acta, 23* (1978) 299–304.
14 E. Santos and M.C. Giordano, *Electrochim. Acta, 30* (1985) 871–878.
15 F. Kadirgan, B. Beden and C. Lamy, *J. Electroanal. Chem., 136* (1982) 119–138.
16 G. Kokkinidis and D. Jannakoudakis, *J. Electroanal. Chem., 153* (1983) 185–200.
17 N.W. Smirnova, O.A. Petrii and A. Grzejdziak, *J. Electroanal. Chem., 251* (1988) 135–152.
18 F. Kadirgan, B. Beden and C. Lamy, *J. Electroanal. Chem., 143* (1983) 135–152.
19 A.A. El-Shafei, S.A. Abd El-Maksoud and M.N.H. Moussa, *J. Electroanal. Chem., 336* (1992) 73–83.
20 T. Biegler, D.A.J. Rand and R. Woods, *J. Electroanal. Chem., 29* (1971) 269–277.
21 D.A.J. Rand and R. Woods, *J. Electroanal. Chem., 31* (1971) 29–38.
22 D.A.J. Rand and R. Woods, *J. Electroanal. Chem., 44* (1971) 83–89.
23 P. Ocon, B. Beden and C. Lamy, *Electrochim. Acta, 32* (1987) 1095–1987.
24 R. Amadelli, N. Markovic, R. Adzic and E. Yeager, *J. Electroanal. Chem., 159* (1983) 391–412.
25 J.W. Schultze and K.J. Vetter, *J. Electroanal. Chem., 44* (1973) 63–81.
26 R.R. Adzic, D.N. Simic, A.R. Despic and D.M. Drazic, *J. Electroanal. Chem., 80* (1977) 81–89.
27 N. Xonoglou, I. Moumtzis and G. Kokkinidis, *J. Electroanal. Chem., 237* (1987) 93–104.
28 A. Castroluna, T. Iwasita and W. Vielstich, *J. Electroanal. Chem., 196* (1985) 301–314.
29 B. Beden, F. Kadirgan, C. Lamy and J.M. Leger, *J. Electroanal. Chem., 142* (1982) 171–190.